

A PROBLEM IN PHOTOELASTICITY

by

TSU-JIUNN PENG

B. S., National Taiwan University, 1960

A MASTER'S REPORT

submitted in partial fulfillment of the

requirements for the degree

MASTER OF SCIENCE

Department of Applied Mechanics

KANSAS STATE UNIVERSITY
Manhattan, Kansas

1964

Approved by:

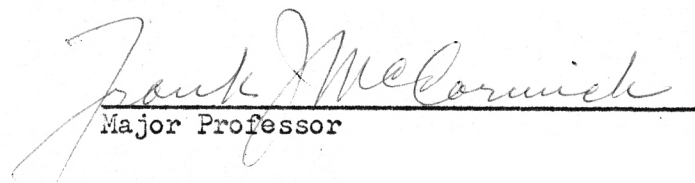

Major Professor

TABLE OF CONTENTS

INTRODUCTION 1

A BRIEF THEORY OF LIGHT 1

 Nature of Light 1

 Polarized Light 3

 Double Refraction 4

THEORY OF TWO-DIMENSIONAL PHOTOELASTICITY 5

 Isoclinics 8

 Isochromatics 8

 Shear Difference Method 10

INVESTIGATION OF MODEL 12

DISCUSSION 38

CONCLUSION 42

ACKNOWLEDGEMENTS 43

REFERENCES 44

INTRODUCTION

Photoelasticity is the science which deals with the effects of stress upon polarized light traversing transparent materials. During the past few decades, much progress has been made in the photoelastic method of stress analysis, it is a rather good tool for experimental stress analysis.

The purpose of this experiment was to investigate the stress distribution of a pinched rectangular beam along the horizontal and vertical axes of symmetry (see Fig. 13).

In the following section, the fundamental theory of two dimensional photoelasticity and experimental procedures will be discussed. As the method of photoelasticity depends fundamentally upon the properties of light, a brief explanation of the theories of light which are relevant will be given in the first section. In the next section, the theory of two-dimensional photoelasticity will be reviewed briefly. The third section includes the procedures of experimental work and description of apparatus. The last section will compare the stress distribution in the rectangular beam and in the circular disk. The circular disk has a diameter equal to the depth of beam, and the stress distribution will be calculated according to two-dimensional theory of elasticity.

A BRIEF THEORY OF LIGHT

Nature of Light

There are two basic theories that attempt to explain the behavior of light. One theory states that the energy is emitted from a light source in the form of discrete quantities; this is the corpuscular, the emission or

particle theory. The second theory stated by Maxwell is that the light energy is transmitted by means of an electromagnetic wave train; this theory is called electromagnetic theory or wave theory of light. Since the transverse wave theory suffices adequately to explain the fundamental facts of photo-elasticity we shall assume this theory as a basis of explanation [5].

From the point of view of the wave theory, ordinary light and also ordinary monochromatic light can be thought of as random or chaotic harmonic vibrations of ether particles in directions transverse to the axis of propagation, i.e., transverse to the direction of the light beam.

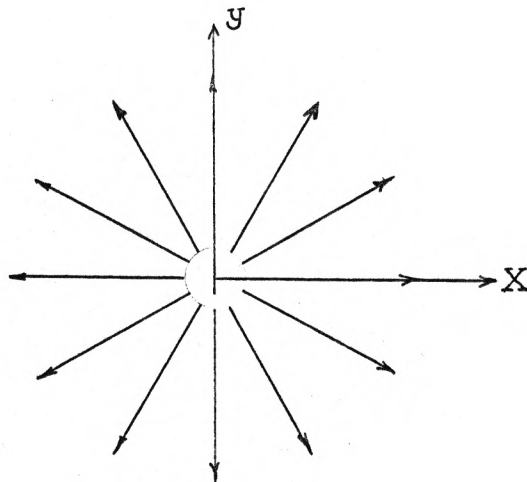


Fig. 1. Idealized representation of light vector.

Ordinary or non-polarized light can be graphically represented by a sketch such as shown in Fig. 1 in which the radius vectors represent the amplitude of the ether vibration.

Polarized Light

Figure 1 represents a cross section of a beam of ordinary light. Such a beam shows no special characteristic when viewed sidewise. Looked at from the x axis, it represents the same picture as when viewed from the y axis. It has no polarity. It is possible to dampen it to eliminate all vibrations except those parallel to one plane, say the X-Z plane. When such is the case, we say that the light is polarized and that the vibrations are in the X-Z plane. Such polarized light is called "plane polarized light" and the X-Z plane may be called the "plane of polarization" [1, 2, 4, 5].

In polarized light, the vibrations of the ether particles are not chaotic or random, but have order and direction. We also distinguish between plane polarized light, circularly polarized and elliptically polarized light. In plane polarized light (Fig. 2a), the transverse vibrations lie wholly in one plane. Not so in circularly polarized light. Here the plane of vibration changes its direction as the ray advances, so that the arrows representing the vector amplitudes of vibration trace out a circle with center at O (Fig. 2b). Lastly, in elliptically polarized light the vibrations change in magnitude as well as direction, in such manner that the vector representing the vibration traces out a definite ellipse (Fig. 2c) [1].

Plane polarized light can be obtained by letting the beam of light pass through a transparent medium such as a Nicol's prism, or more usually a Polaroid Sheet.

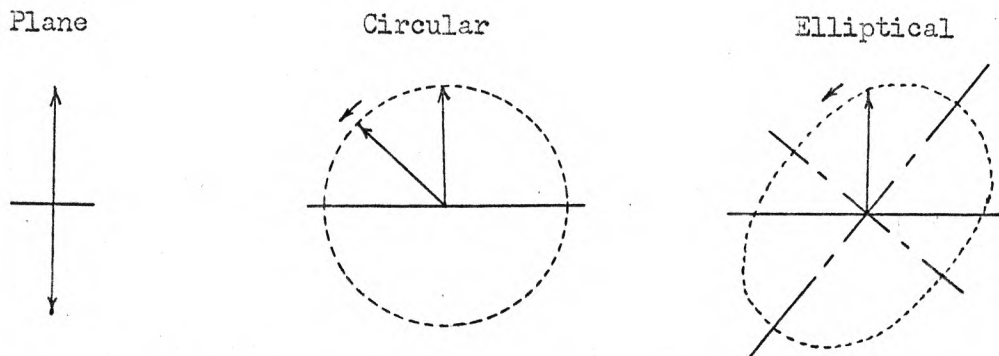


Fig. 2. Vector representation of polarized light.

(a) Plane Polarized

(b) Circular Polarized

(c) Elliptically
Polarized

Double Refraction

The fundamental optical phenomenon entering into all photoelastic investigations of stress distribution is the phenomenon of "double refraction". Not only does this account for what is going on within the stressed model itself, but it also forms the basis for the design of the central parts (such as quarter-wave plates) of all effective photoelastic polariscopes.

Numerous transparent solids, such as quartz, mica or Iceland spar, have two or three optical axes; mica, due to the distribution of molecules, has two optical axes which are in planes parallel to the cleavage planes of the crystal and are at right angles to each other. Therefore, when a beam of monochromatic light is incident upon a sheet of mica, it splits into two plane polarized waves; the ordinary and the extraordinary, which vibrate in mutually perpendicular planes. The two beams travel through the crystal with different velocities and therefore emerge with a phase difference whose magnitude is dependent upon the thickness of the crystal and the difference of refraction indices in the two mutually perpendicular planes [2, 4, 5].

Due to mica having this special character, a sheet of mica is often used as a "quarter-wave plate" by adjusting the thickness of the sheet so that the relative retardation between the two components of the light is exactly one quarter of one wave length for a certain monochromatic light.

THEORY OF TWO-DIMENSIONAL PHOTOELASTICITY

Photoelasticity is based on the fact that an optically isotropic transparent solid becomes optically anisotropic when subjected to forced deformation, that is, a deformed optically isotropic solid demonstrates optical properties similar to those of crystals and the degree of optical anisotropy is proportional to the deformation of the material.

Experiment has shown that at any point in a stressed transparent solid, the axes of polarization of light passing through the solid are parallel to the directions of the principal stresses in the plane of the wave-front at that point, also the difference of the velocities of the two oppositely polarized waves at the point is proportional to the difference of these two principal stresses [2, 4, 5].

In Fig. 3, abcd represents a deformed transparent material of uniform thickness which is set perpendicular to the line of propagation of plane polarized light. O is the point of intersection of the plate and the polarized light.

$$A_1 = a \cos \theta \sin \omega t$$

$$A_2 = a \sin \theta \sin \omega t$$

If d is the thickness of the plate, the time difference between two components of light will be

$$\delta t = \frac{d}{c} (n_1 - n_2)$$

The relative retardation between the two components of the light expressed in whole wavelengths of the light may be written as

$$\omega \delta t = 2\pi F = \frac{2\pi d}{\lambda} (n_1 - n_2)$$

or

$$F = \frac{d}{\lambda} (n_1 - n_2)$$

where $\lambda = 2\pi c/\omega$ is the wave length of light and F is the number of wavelengths of relative retardation.

Experiment has shown that the difference of these velocities of light is proportional to the difference in the principal stresses, therefore, the relation between them will be shown as

$$F = \frac{d}{\lambda} (n_1 - n_2) = \frac{d}{C} (P - Q)$$

where C is called the photoelastic constant of the transparent material [2, 4, 5].

The resultant amplitude of the emergent light in plane mn because of relative retardation would be

$$A_5 = a \sin 2\theta \sin \frac{\pi d}{C} (P - Q) \cos (\omega t + \frac{\pi d}{C} (P - Q))$$

or

$$A_5 = a \sin 2\theta \sin F\pi \cos (\omega t + F\pi)$$

This is a simple harmonic vibration with amplitude $a \sin 2\theta \sin F\pi$. Thus the intensity of the light will be zero if either $\sin 2\theta$ or $\sin F\pi$ is zero, i.e., if either $2\theta = n\pi$ or $F\pi = n\pi$ where n is zero or an integer [5].

Isoclinics

When the amplitude becomes zero because $2\theta = n\pi$, the principal stresses in the plate are parallel to the planes OA and mn respectively. If the planes of OA and mn are coincident with the axes of the polarizer and analyzer which are crossed, the intensity of light emerging from the analyzer will be zero. At every point in the plate where this occurs, the intensity of light transmitted will be zero, whatever the wave length and whatever the magnitude of $(P - Q)$. In such case, certain black regions or lines will be observed which show the locus of all points in the plate at which the directions of the principal stresses are parallel to the axes of the polarizer and analyzer. These black regions are called "Isoclinic lines" or "lines of constant inclination of the principal stress" or simply "isoclinics" [2, 4, 5].

From the elementary theory of elasticity, we know the directions of the principal stresses will change from point to point continuously in the area of the plate, therefore, if polarizer and analyzer are rotated simultaneously, still keeping them crossed, the isoclinics will move from point to point continuously where the principal stresses are parallel to the new direction of the polarizer and analyzer. Thus we shall get a different set of isoclinic lines for each different orientation of polarizer and analyzer.

Isochromatics

The second condition for zero intensity of transmitted light occurs when the argument of the sine term $F\pi$ is either zero or π multiplied by an integer. This means F is either zero or an integral number of wave lengths of the light employed. If monochromatic light is employed, in this condition

certain black lines or regions will be observed. The lines or regions are called "isochromatic fringes" or "lines of constant color", "lines of constant principal stress difference", "lines of constant maximum shear stress" or simply "isochromatics" [7, 8].

In a stressed plate two distinct sets of dark fringes--isoclinics and isochromatics are usually viewed from a plane polariscope, in such cases the isoclinics always tend to mask the isochromatics. In order to eliminate the isoclinics, the quarter-wave plates are used. Due to introducing the quarter-wave plates, the arrangement of polarizer, analyzer and quarter-wave plates will produce circularly polarized light, and this kind of arrangement is called a "circular polariscope", as distinguished from plane polariscope [2, 4, 5]. In the isochromatic pattern, showing the lines of relative retardation, the fringe order frequently cannot be interpreted without some indication of the growth of the pattern as the loading was applied. Therefore, the growing fringe pattern must be watched as the loading is applied, and notes taken on the fringe order at various critical points. With this information available, the fringes on the photograph of the fringe pattern can be easily labeled for the analysis. Frequently the position of the zero fringe is all that is necessary to give the key to the fringe-value distribution in the pattern.

The fringe pattern offers merely the information of the difference of principal stress ($P - Q$) which is not enough to determine the principal stress at certain points, therefore it is necessary to know the direction of the principal stress at that point for separating stresses. The isoclinic pattern will give the whole information of the direction of principal stress.

$$\tau_{xy} = \frac{p - q}{2} \sin 2\theta = (p - q) \frac{1}{2} \sin 2\theta' \quad (1)$$

where p is algebraically larger than q , and θ' is measured from the normal N to the direction of the algebraically maximum principal stress p . From the above description, we observe that the direction of the shear stress τ_{xy} is the same as the initial direction of the angle θ' [2].

The equilibrium equation of two dimensions in theory of elasticity is given as

$$\frac{\partial \sigma_x}{\partial x} + \frac{\partial \tau_{xy}}{\partial y} = 0 \quad (2)$$

$$\frac{\partial \sigma_y}{\partial y} + \frac{\partial \tau_{xy}}{\partial x} = 0$$

Using axes as shown in Fig. 5 and integrating the first Eq. (2), it follows that

$$(\sigma_x)_p = (\sigma_x)_0 - \int_0^p \frac{\partial \tau_{xy}}{\partial y} dy \quad (3)$$

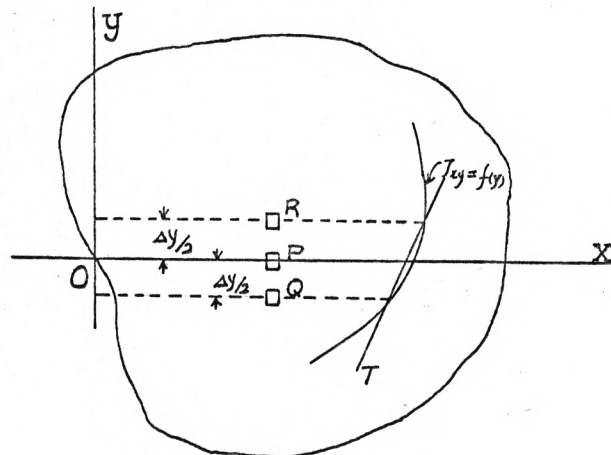


Fig. 5.

in which $(\sigma_x)_p$ and $(\sigma_x)_0$ denote respectively the stresses at points P and O.

By means of approximation, the Eq. (3) may be expressed as

$$(\sigma_x)_p = (\sigma_x)_0 - \sum_0^p \frac{\Delta T_{xy}}{\Delta y} \Delta x \quad (4)$$

where ΔT_{xy} is difference of shear stress at R and Q along a line $X = P$, then $\Delta T_{xy}/\Delta y$ is an approximation to the slope of the curve $f(y)$ at point P along a line parallel to Y axis.

Selecting a suitable interval Δx and Δy , we will get an approximate value $(\sigma_x)_p$ along X axis if we can determine the value of $(\sigma_x)_0$ at boundary.

INVESTIGATION OF MODEL

The photoelastic polariscope used in the experimental stress analysis is sketched in Fig. 6, it is an 8 inch Research Polariscope manufactured by Chapman Laboratories. All components and controls of this equipment are mounted on a single rigid steel tube that extends the length of the polariscope.

In regard to the light source, there is a dual lamp housing which contains both white and monochromatic light sources and is mounted so that either source may be selected. The white source is a ribbon filament incandescent lamp and the monochromatic source is a high intensity mercury vapor lamp equipped with glass filter passing the green line (5461\AA).

The material selected for the model was CR-39 (Allyl Diglycol Carbonate) which has high optical sensitivity and less susceptibility to time-edge effect than other materials.

The mechanical properties of CR-39 as given by Heywood [3] are: elastic limit = 3,000 psi, ultimate strength = 7,000 psi and Young's Modulus = 250,000 psi. Some of the disadvantages of CR-39 are its tendency to creep

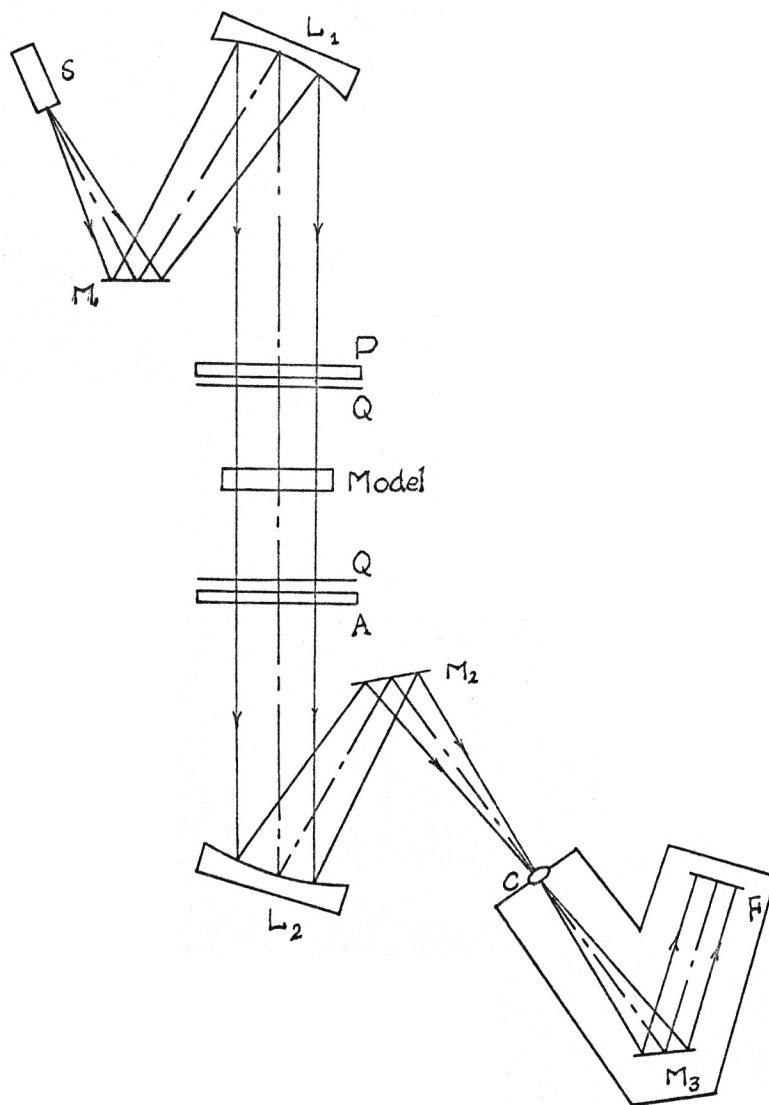


Fig. 6. Sketch of photoelastic polariscope.

S - light source

P - polaroid

M - plane mirror

A - polaroid

L - parabolic mirror

C - camera lens

Q - quarter-wave plate

F - film holder

under load and the effect of temperature on the physical and optical properties of the materials. However, most transparent plastics have these disadvantages, so the experiment must be done in a few hours after the model is machined.

To make a suitable model, a Dremel Moto-Saw was employed for a rough cut. Then a high speed milling machine (Chapman Model Making Kit, Model 45) was used for the finished cut. A 0.1 inch thick brass template was first made according to the exact contour required. The template was then placed on a sheet of CR-39 and a pencil was used to outline the model on the plastic. The template was securely attached to the model with double-coated adhesive tape. The plastic sheet was carefully cut to leave about 1/16 inch margin around the desired boundary by using the mechanical saw. The final milling operation was achieved in the manner of a series of fast, light cuts, until the template was in contact with the guide pin as shown in Fig. 7.

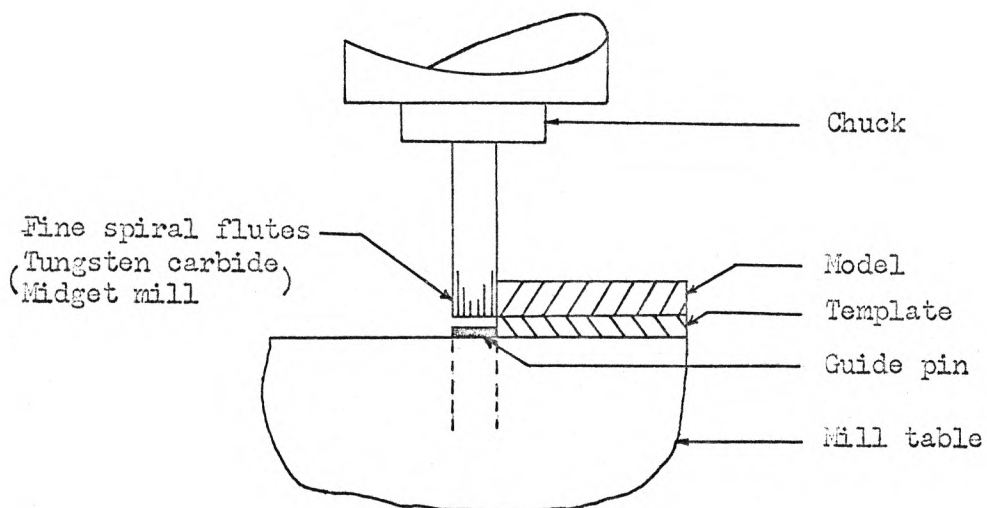


Fig. 7. Sketch of milling machine.

The next step was the calibration of the material CR-39. The fringe number at various sections of a three-stage tension model for several loads were recorded. The sketch of the three-stage tension model is shown in Fig. 8; the data are shown in Table 1. These data are used to plot a curve with the stress as the ordinate and fringe number as the abscissa, the curve is shown in Fig. 8. The fringe-stress coefficient found from the slope of this curve is 373 pounds per square inch per fringe.

Table 1. Data taken for the determination of fringe-stress coefficient by use of a three-stage tension model.

Load in pounds	Fringe number Sect. A	Stress (psi) Sect. A	Fringe number Sect. B	Stress (psi) Sect. B	Fringe number Sect. C	Stress (psi) Sect. C
		Area = 0.045 sq.in.		Area = 0.061 sq.in.		Area = 0.094 sq.in.
16.45	1	367				
22.78			1	374		
32.9	2	732				
35.4					1	376
44.3			2	740		
50.6	3	1149				
67.01	4	1490				
68.25			3	1120		
69.55					2	740
82.2	5	1829				

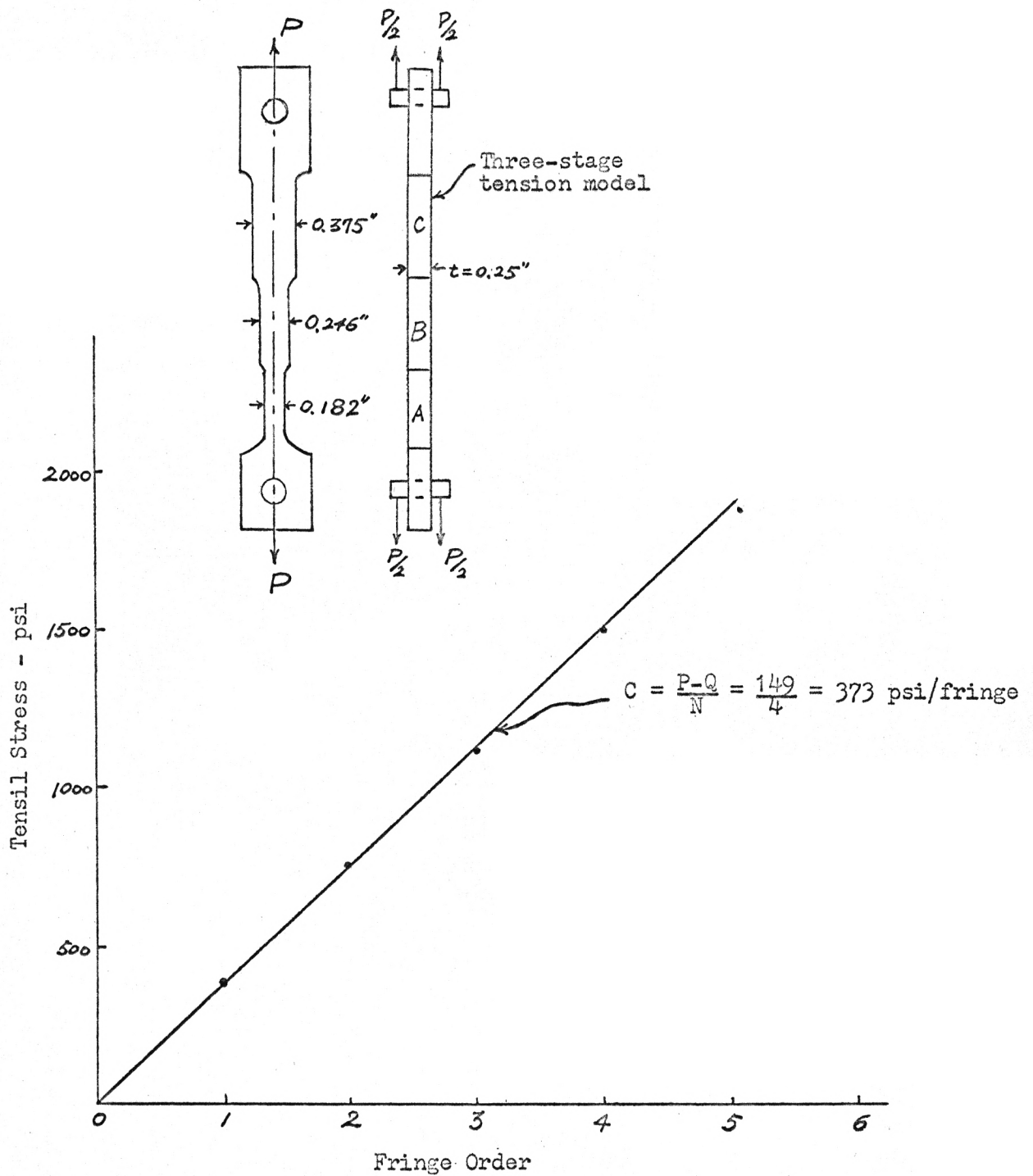


Fig. 8. Sketch of three-stage tension model and the curve of stress-optical coefficient.

After the rectangular model was machined, the model was placed in a loading frame and investigated in the polariscope. The model was loaded by means of a loading jig as shown in Fig. 9. The load was applied to the loading jig through a loading spring. The applied load was measured and indicated by a dial indicator on the spring. The jig was located on the polariscope midway between the polarizer and the analyzer.

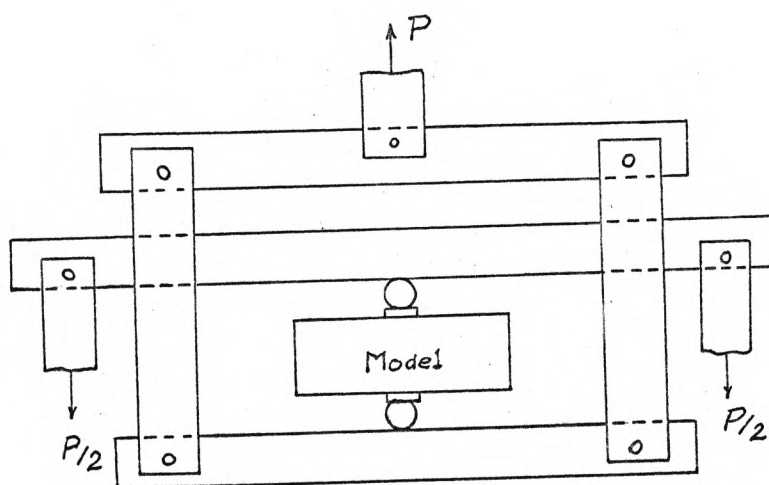
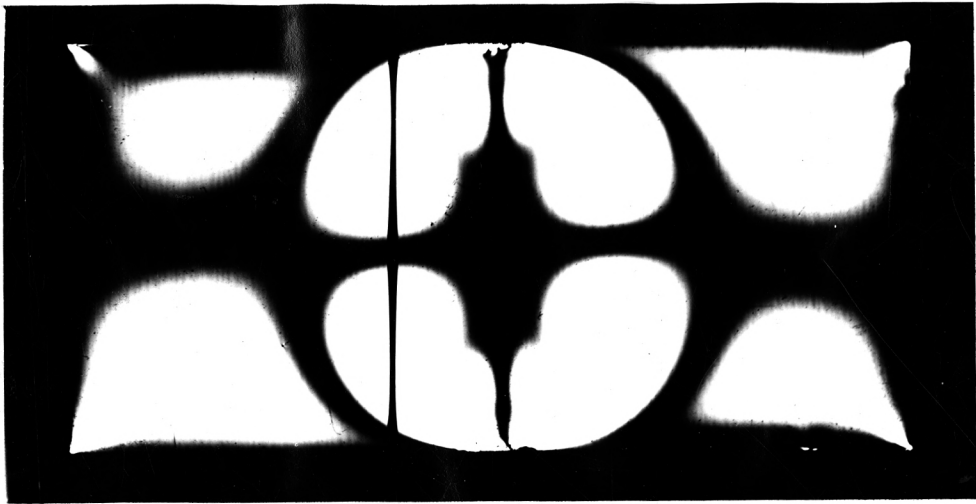
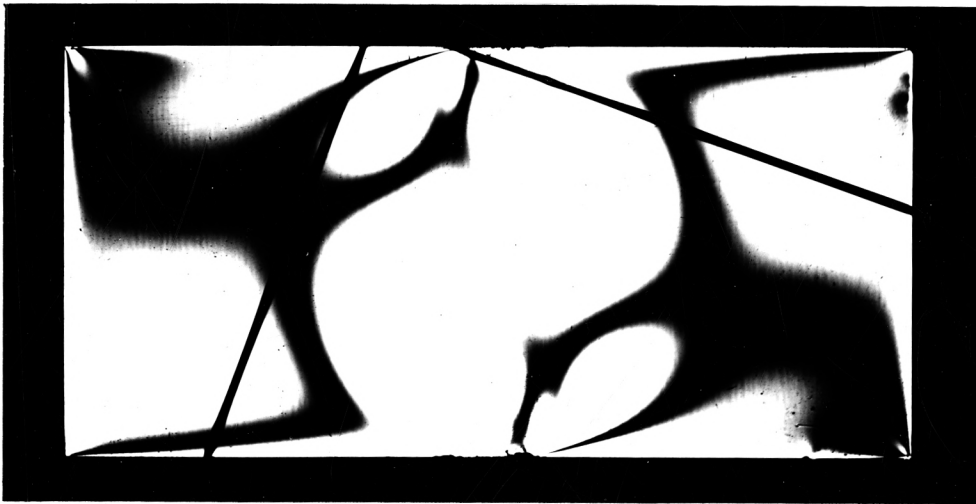


Fig. 9. Sketch of loading jig.

The simplest kind of a polariscope consists of a light source and two polaroid sheets which produces "plane polarized light". The polarized sheet nearest the light source is called the polarizer and the next polaroid sheet the analyzer as shown in Fig. 6. These can be crossed or parallel depending upon whether a light or dark field is desired. A crossed polarizer and analyzer which completely extinguishes the light was employed to investigate the isoclinics. The ordinary white light was employed to investigate the isoclinics. The isoclinic pattern is shown in Figs. 10 and 11.



(a) 2° isoclinic.



(b) 21° isoclinic.

Fig. 10. Photographs of isoclinics in a rectangular beam.

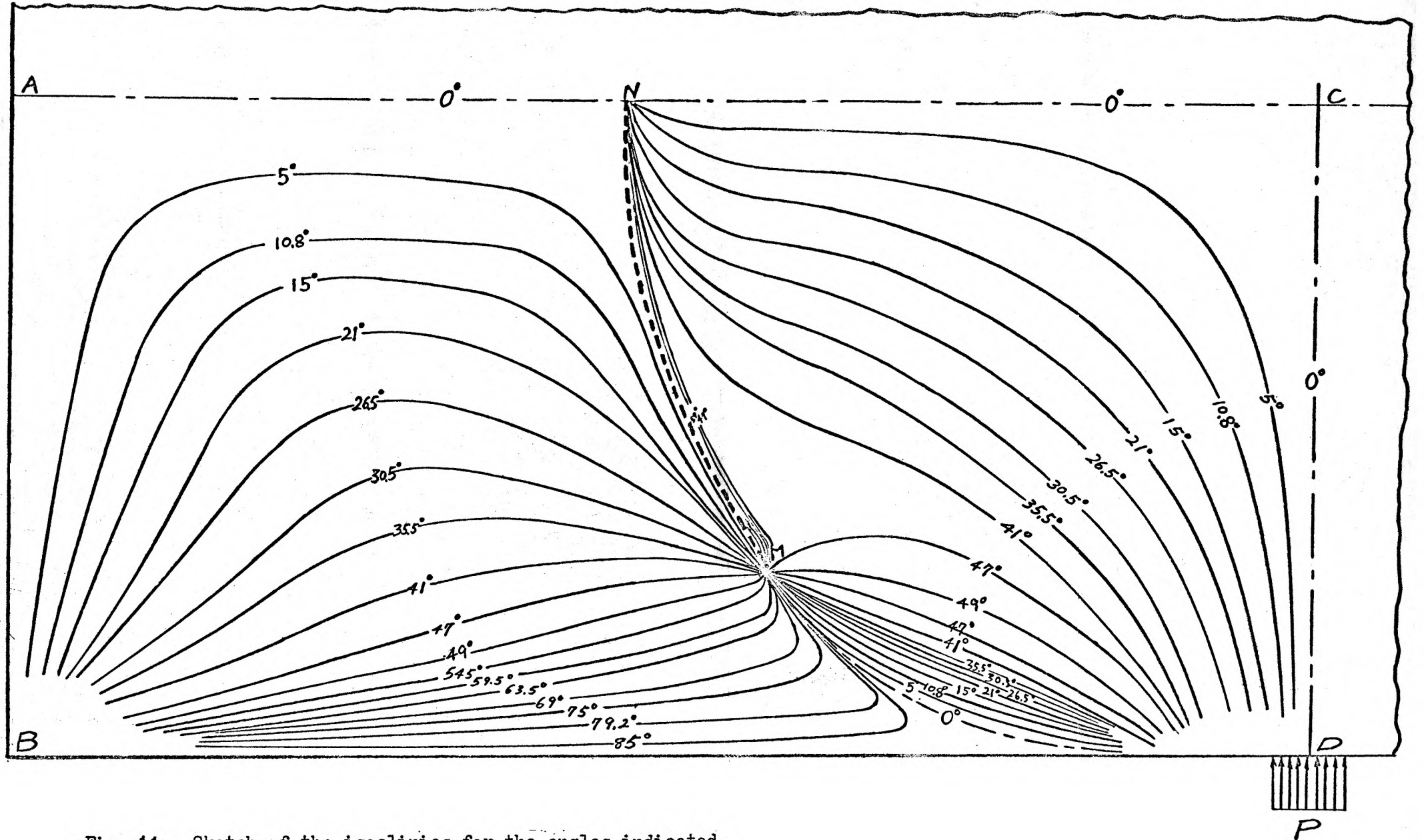


Fig. 11. Sketch of the isoclinics for the angles indicated.

To investigate isochromatics, circularly polarized light was employed with monochromatic light. Two quarter-wave plates were set between the analyzer and polarizer with the axis making angles of 45 degrees to the axis of analyzer and polarizer to produce the circularly polarized light. The typical fringe pattern is shown in Fig. 12.

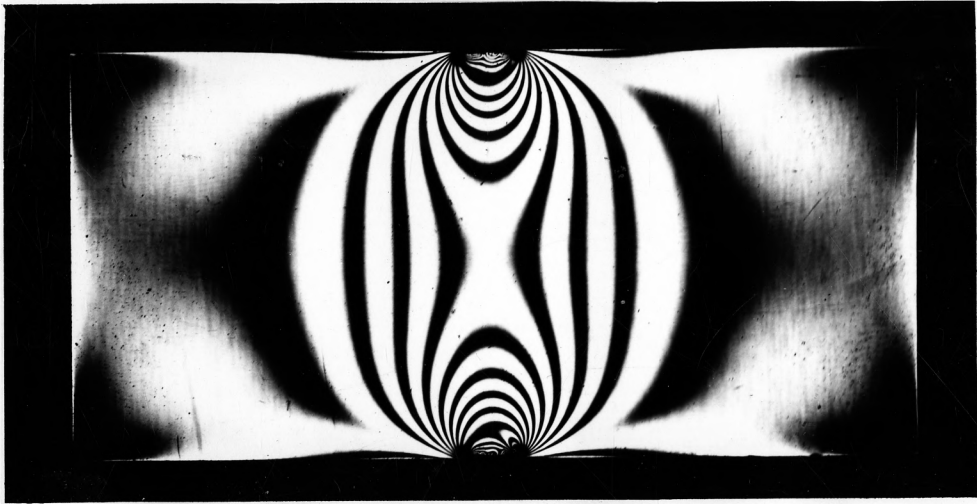
With the arrangement of the polariscope mentioned previously, a complete photographic record of the results was made. The camera was equipped with a standard press back which accommodated standard 4" x 5" film holders. When the back of the camera was open, an image of the stressed model could be viewed on the ground glass.

The isochromatic photographs were taken on Kodak Contrast Process Panchromatic Film with an exposure time of one second. The negatives were developed for 3 to 4 minutes in Kodak D-11 Developer. The same film was used for the isoclinic photographs, but these were exposed for 1/2 second. The load was changed slightly to make the isochromatics less distinct than before, while taking photographs of the isoclinics. The reason for slight loading is that the principal stress directions are defined no matter how great the load is. The negatives were then developed as before.

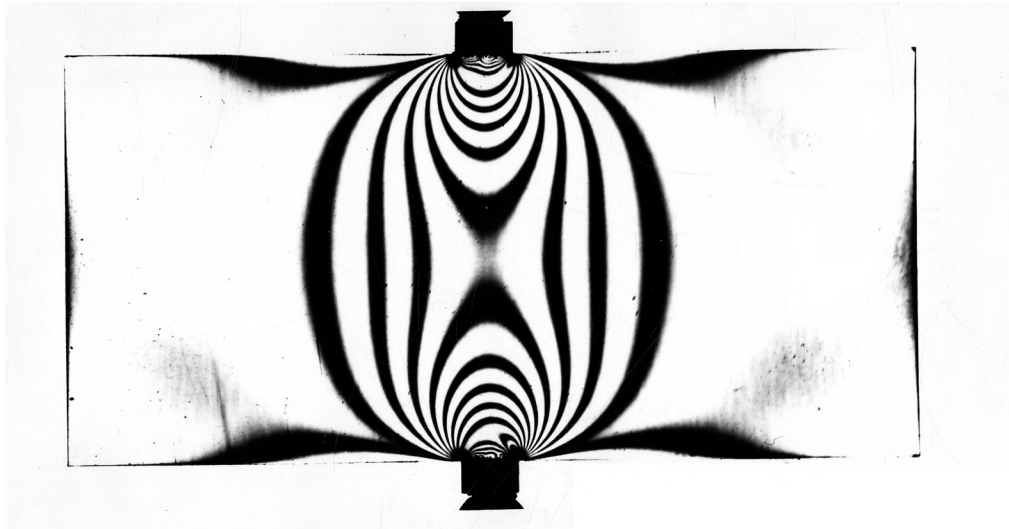
The following method, which is called the Tardy Method, was used to measure fractional fringe order. This procedure is outlined below:

1. Determine the direction of principal stress at point A which is in question. Then rotate the crossed analyzer and polarizer simultaneously until a dark line covers the point A. At that time, the polarizer and the analyzer are parallel to the directions of principal stress at A.

2. Insert quarter-wave plates to produce circularly polarized light of dark field. In this arrangement, the polarizer and the two quarter-wave



a. Dark-field polariscope.



b. Light-field polariscope.

Fig. 12. Isochromatic fringe pattern of a rectangular beam.

plates are locked in position. Then rotating the analyzer through 180 degrees results in a motion corresponding to one complete fringe.

3. Rotate the analyzer to extinguish light at A. The angle of rotation of the analyzer θ in degrees is measured and $\theta/180$ is the fractional fringe at that point. Turning the analyzer in one sense results in an increase in the fringe number and rotating it in the opposite sense decreases the fringe order at that point. For instance, at a point A lying between fringe order one and two, the number of fractional fringe is either $(1 + \theta_1/180)$ or $(2 - \theta_2/180)$.

The procedures to separate the stresses both on the vertical axis DC and horizontal axis AC of symmetry of the beam as shown in Fig. 13 were carried out in the following manner.

First only the quarter ABCD of beam was considered, because of its symmetry to the other three parts, then line AB was divided into ten equal intervals which had the length of $d/20$ and the horizontal lines were drawn to get sections a-a, b-b, c-c, etc. In the same manner horizontal AC was divided into ten equal intervals of length $2d/20$ and the vertical lines were drawn parallel to line AB to get lines 0-0, 1-1, 2-2, etc. as shown in Fig. 14.

The fringe order and the direction of principal stress at each point on every horizontal section were determined from the fringe pattern and isoclinic pattern. The direction and the magnitude of shear stress at each point of a section were determined by using the Eq. (1) and the stress trajectories shown in Fig. 15. The direction and magnitude of shear stress along every section were tabulated in Tables 2, 3, and 4.

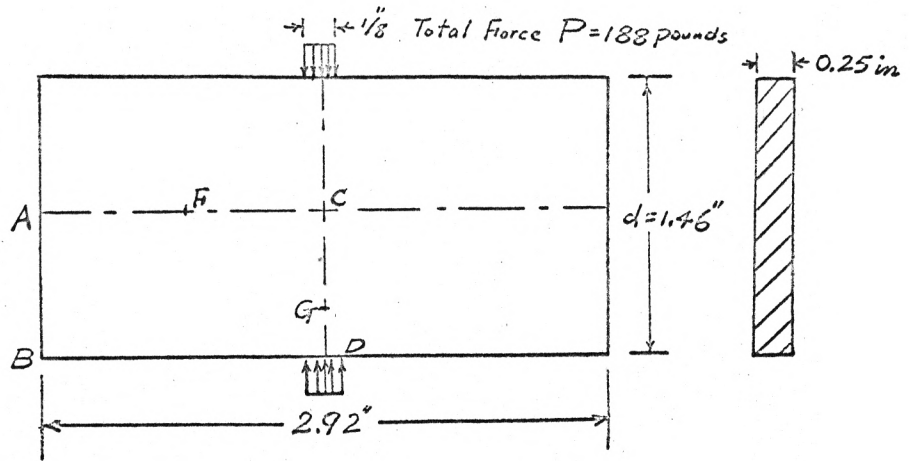


Fig. 13. Dimension of rectangular beam.

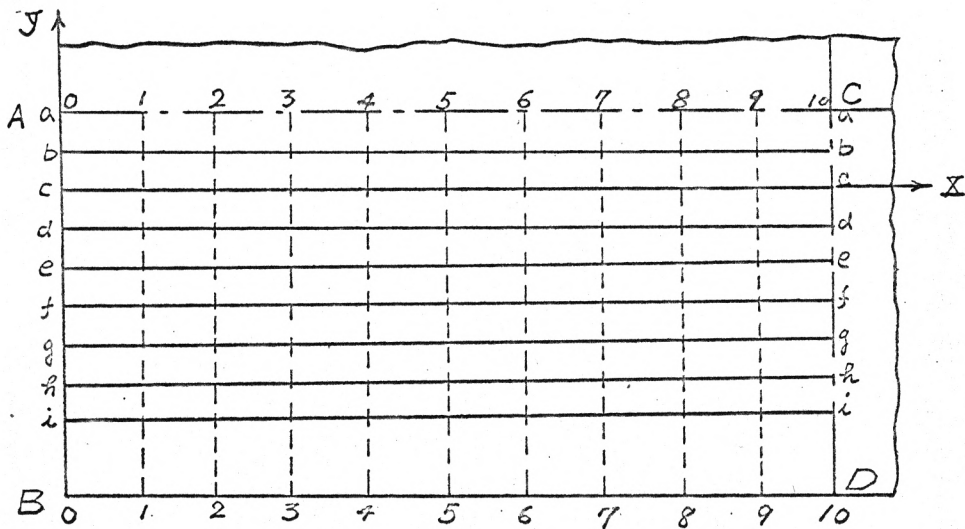


Fig. 14. The enlargement of ABCD section on Fig. 13.

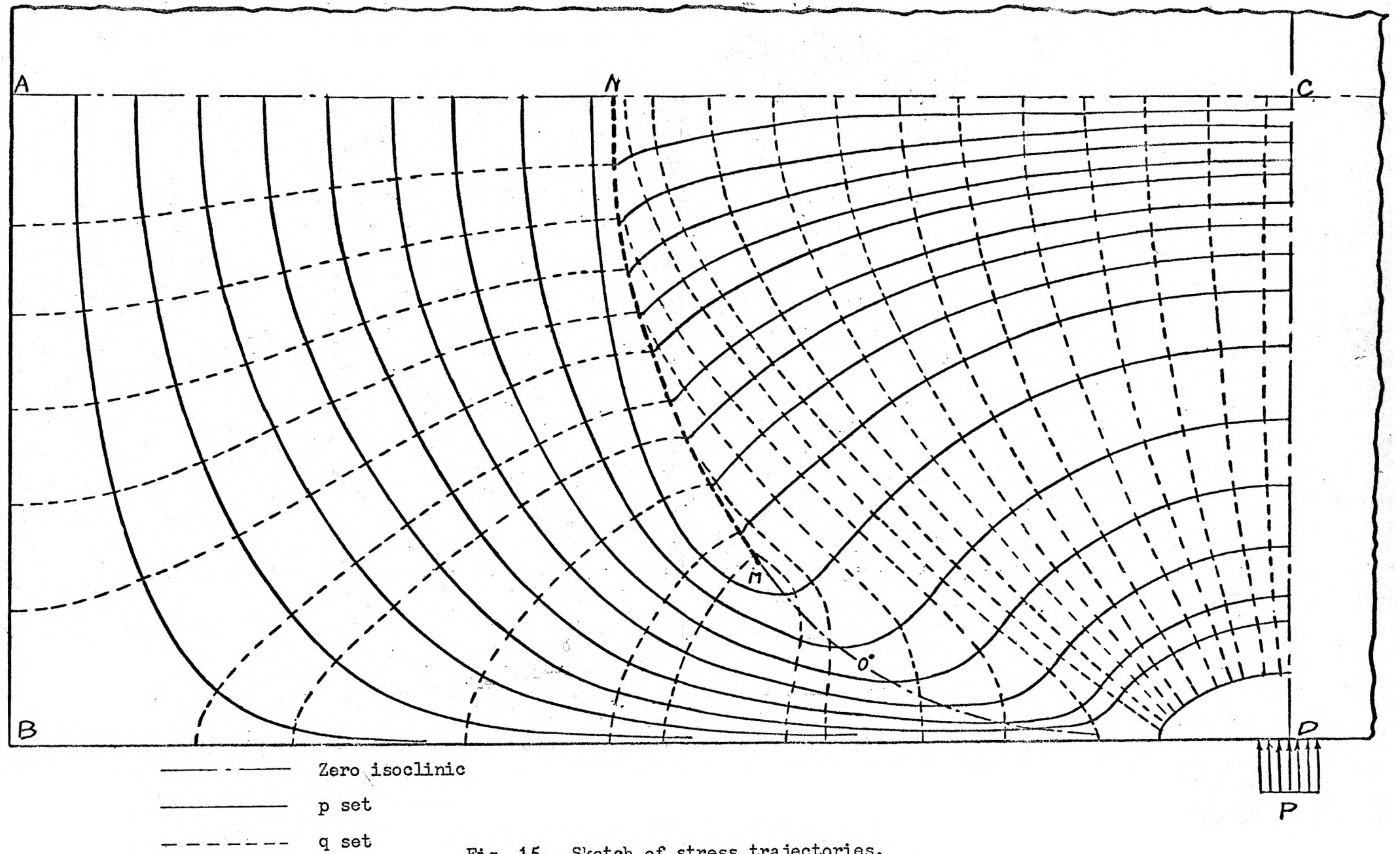


Fig. 15. Sketch of stress trajectories.

Using the data shown in Tables 2, 3, and 4, we may calculate the normal stresses along horizontal sections by means of the shear difference method. For instance, we take section c-c as the X axis and AB as the Y axis, then we can apply the Eq. (4) where ΔT_{xy} is the shear difference between section b-b and d-d and Δx is equal to Δy (see Fig. 14). The Eq. (4) becomes

$$(\sigma_x)_p = (\sigma_x)_c - \sum_{n=0}^{n=10} \Delta T_{xy} \cdot 1 \quad (5)$$

Table 6 shows the value of the normal stress σ_x at points along section c-c. Similarly, Tables 5-11 show the value of the normal stress σ_x at points along each section.

To calculate σ_y along CG, we use the equation $y = \sigma_x \pm \sqrt{(p-q)^2 - 4T_{xy}^2}$. The value of the normal stress σ_y at points along CG is shown in Table 13. In the same manner, the value of normal stress σ_y along AC was obtained and shown in Table 14.

Table 2. Calculation of transverse shear-stress across section of a rectangular beam.

Sta- tion	ϕ deg.	$\frac{1}{2} \sin 2\phi$	Sect. a-a fringes		ϕ deg.	$\frac{1}{2} \sin 2\phi$	Sect. b-b fringes		ϕ deg.	$\frac{1}{2} \sin 2\phi$	Sect. c-c fringes	
			p-q	T_{xy}			p-q	T_{xy}			p-q	T_{xy}
0	0	0	0.20	0	0	0	0.2	0	0	0	0.2	0
1	0	0	0.18	0	3.5	0.061	0.05	-0.003	5.5	0.095	0.04	-0.004
2	0	0	0.16	0	4.5	0.078	0.05	-0.004	9	0.105	0.03	-0.003
3	0	0	0.15	0	4.5	0.078	0.05	-0.004	10	0.171	0.02	-0.004
4	0	0	0.09	0	3.5	0.061	0.01	-0.001	8	0.138	0.01	-0.002
5	0	0	0.2	0	21.5	0.341	0.15	-0.051	30.5	0.437	0.01	-0.005
6	0	0	0.5	0	10	0.17	0.40	0.068	18	0.294	0.45	0.132
7	0	0	1.1	0	7.0	0.12	1.0	0.12	14.5	0.242	1.1	0.266
8	0	0	2.0	0	6.0	0.11	2.0	0.22	12.5	0.212	2.1	0.445
9	0	0	2.85	0	3.0	0.06	2.8	0.16	7.5	0.13	2.95	0.284
10	0	0	3.35	0	0	0.00	3.3	0	0	0.0	3.45	0.0

Table 3. Calculation of transverse shear-stress across sections of a rectangular beam.

Sta- tion	Sect. d-d		Sect. e-e		Sect. f-f		Sect. d-d		Sect. e-e		Sect. f-f	
	ϕ deg.	$\frac{1}{2} \sin 2\phi$	p-q	T_{xy}	ϕ deg.	$\frac{1}{2} \sin 2\phi$	p-q	T_{xy}	ϕ deg.	$\frac{1}{2} \sin 2\phi$	p-q	T_{xy}
0	0	0	0	0	0	0	0	0	0	0	0	0
1	9.5	0.163	0.02	-0.003	10.8	0.18	0.02	-0.004	12.5	0.212	0.04	-0.008
2	15.5	0.26	0.10	-0.026	20	0.322	0.06	-0.019	24.5	0.377	0.09	-0.034
3	17.0	0.28	0.08	-0.022	24	0.372	0.06	-0.022	28.5	0.42	0.16	-0.067
4	14.5	0.242	0.02	-0.004	21	0.335	0.02	-0.007	26.5	0.40	0.09	-0.036
5	80.0	0.171	0.00	0	7	0.121	0.01	-0.001	13	0.419	0.02	-0.008
6	29	0.424	0.4	0.169	37	0.48	0.4	0.192	46	0.5	0.25	+0.125
7	23	0.36	1.05	0.37	28.5	0.42	1.0	0.42	35.5	0.473	0.9	+0.426
8	15	0.25	2.05	0.5	22	0.347	2.05	0.71	27.5	0.405	2.0	+0.83
9	10	0.17	3.05	0.51	12	0.203	3.3	0.67	17.5	0.283	3.5	0.99
10	0	0	3.65	0	0	0.0	3.93	0.0	0	0	4.4	0

Table 4: Calculation of transverse shear-stress across section of rectangular beam.

Sta- tion	ϕ deg.	$\frac{1}{2} \sin 2\phi$	Sect. g-g fringes		ϕ deg.	$\frac{1}{2} \sin 2\phi$	Sect. h-h fringes		ϕ deg.	$\frac{1}{2} \sin 2\phi$	Sect. i-i fringes	
			p-q	T_{xy}			p-q	T_{xy}			p-q	T_{xy}
0	0	0	0	0	0	0	0	0	0	0	0	0
1	15	0.25	0.04	-0.01	21	0.335	0.03	-0.010	27	0.405	0.03	-0.012
2	28	0.415	0.1	-0.042	32	0.45	0.10	-0.045	35.5	0.475	0.09	-0.042
3	33	0.457	0.16	-0.074	37.5	0.483	0.18	-0.087	44	0.494	0.26	-0.13
4	32	0.449	0.14	-0.063	40	0.493	0.17	-0.084	47	0.498	0.15	-0.07
5	26	0.394	0.08	-0.032	42.5	0.498	0.04	-0.02	37	0.478	0.08	-0.037
6	82	0.138	0.15	0.020	35	0.470	0.1	+0.047	10	0.171	0.01	0.002
7	43.5	0.499	0.85	0.425	50	0.49	0.7	-0.343	42	0.49	0.30	0.147
8	33	0.457	2.05	0.945	41.5	0.497	1.85	+0.92	48	0.498	1.5	0.75
9	22	0.35	3.83	1.34	27.5	0.41	4.2	+1.73	44	0.499	4.5	2.25
10	0	0	5.0	0	1.0	0.009	6.1	0.054	1.5	0.03	7.75	0.233

Table 5. Calculation of transverse normal stress at points at section a-a.

Station	ΔT_{xy} fringe	Mean ΔT_{xy} fringe	Mean $\Delta T_{xy}(-\frac{\Delta Y}{\Delta X})$	σ_x fringe	σ_x p.s.i.
0	0			0	0
1	+0.012	+0.006	-0.006	-0.006	-2.4
2	+0.012	+0.012	-0.012	-0.018	-6.7
3	+0.008	+0.010	-0.010	-0.028	-10.5
4	+0.002	+0.005	-0.005	-0.033	-12.3
5	+0.102	+0.052	-0.052	-0.085	-31.7
6	-0.13	-0.014	+0.014	-0.071	-26.5
7	-0.24	-0.185	+0.185	+0.114	+42.5
8	-0.44	-0.34	+0.34	+0.454	+169.0
9	-0.32	-0.38	+0.38	+0.834	+312.0
10	0	-0.16	+0.16	+0.994	+370.0

Table 6. Calculation of transverse normal stress at points at section c-c.

Station	ΔT_{xy} fringe	Mean ΔT_{xy} fringe	Mean $\Delta T_{xy}(-\frac{\Delta Y}{\Delta X})$	σ'_x fringe	σ_x p.s.i.
0	0	0	0	0	0
1	0	+0.01	-0.01	0	0
2	+0.022	+0.02	-0.02	-0.01	-3.7
3	+0.018	+0.01	-0.01	-0.03	-11.1
4	+0.003	-0.02	+0.02	-0.04	-14.8
5	-0.054	-0.07	+0.07	-0.02	-7.4
6	-0.100	-0.18	+0.18	+0.05	+18.6
7	-0.26	-0.27	+0.27	+0.23	+86.0
8	-0.28	-0.31	+0.31	+0.50	+186.5
9	-0.35	-0.17	+0.17	+0.81	+302.0
10	0			+0.98	+366.0

Table 7. Calculation of transverse normal stress at points at section d-d.

Station	ΔT_{xy} fringes	Mean ΔT_{xy} fringes	Mean $\Delta T_{xy}(-\frac{\Delta y}{\Delta x})$	σ_x fringes	σ_x p.s.i.
0	0	0	0	0	0
1	0	+0.008	-0.008	0	0
2	+0.016	+0.017	-0.017	-0.008	-3.0
3	+0.018	+0.011	-0.011	-0.025	-9.3
4	+0.005	+0.000	-0.000	-0.033	-12.3
5	-0.004	-0.032	+0.032	-0.33	-12.3
6	-0.060	-0.11	+0.11	-0.001	-0.3
7	-0.154	-0.21	+0.21	+0.11	+41.0
8	-0.265	-0.33	+0.33	+0.32	+119.2
9	-0.396	-0.20	+0.20	+0.65	+242.5
10	0			+0.85	+317.0

Table 8. Calculation of transverse normal stress at points at section e-e.

Station	ΔT_{xy} fringes	Mean ΔT_{xy} fringes	Mean $\Delta T_{xy}(-\frac{\Delta y}{\Delta x})$	ϵ'_x fringes	ϵ'_x p.s.i.
0	0			0	0
1	+0.005	+0.002	-0.002	-0.002	-0.7
2	+0.008	+0.007	-0.007	-0.009	-3.4
3	+0.045	+0.026	-0.026	-0.035	-13.0
4	+0.032	+0.038	-0.038	-0.073	-27.2
5	+0.008	+0.020	-0.020	-0.093	-34.7
6	+0.044	+0.026	-0.026	-0.119	-44.4
7	-0.06	-0.008	+0.008	-0.110	-41.0
8	-0.33	-0.20	+0.20	+0.09	+33.6
9	-0.48	-0.41	+0.41	+0.50	+186.5
10	0	-0.24	+0.24	+0.74	+276.0

Table 9. Calculation of transverse normal stress at points at section f-f.

Station	ΔT_{xy} fringes	Mean ΔT_{xy} fringes	Mean $\Delta T_{xy}(-\frac{\Delta y}{\Delta x})$	σ_x fringes	σ_x p.s.i.
0	0			0	0
1	+0.006	+0.003	-0.003	-0.003	-1.1
2	+0.023	+0.014	-0.014	-0.017	-6.4
3	+0.052	+0.037	-0.037	-0.054	-20.2
4	+0.053	+0.052	-0.052	-0.106	-39.5
5	+0.032	+0.042	-0.042	-0.148	-55.2
6	+0.17	+0.10	-0.10	-0.248	-92.5
7	-0.01	+0.08	-0.08	-0.256	-95.5
8	-0.24	-0.13	+0.13	-0.126	-47.0
9	-0.67	-0.46	+0.46	+0.334	+124.5
10	0	-0.34	+0.34	+0.674	+251.8

Table 10. Calculation of transverse normal stress along section g-g.

Station	ΔT_{xy} fringes	Mean ΔT_{xy} fringes	Mean $\Delta T_{xy}(-\frac{\Delta Y}{\Delta X})$	ϵ_x fringes	ϵ_x p.s.i.
0	0			0	0
1	+0.002	+0.001	-0.001	-0.001	-0.4
2	+0.011	+0.006	-0.006	-0.007	-2.6
3	+0.020	+0.015	-0.015	-0.022	-8.2
4	+0.048	+0.034	-0.034	-0.056	-20.9
5	+0.012	+0.030	-0.030	-0.086	-32.0
6	+0.08	+0.046	-0.046	-0.132	-49.2
7	+0.09	+0.085	-0.085	-0.217	-81.0
8	-0.09	+0	0	-0.217	-81.0
9	-0.74	-0.42	+0.42	+0.21	+78.3
10	-0.054	-0.40	+0.40	+0.61	+227.5

Table 11. Calculation of transverse normal stress along section h-h.

Station	σ_x fringes	Mean ΔT_{xy} fringes	Mean $\Delta T_{xy}(-\frac{\Delta y}{\Delta x})$	σ_x fringes	σ_x p.s.i.
0	0			0	0
1	+0.002	+0.001	-0.001	-0.001	-0.4
2	+0	+0.001	-0.001	-0.002	-0.8
3	+0.05	+0.025	-0.025	-0.027	-10.1
4	+0.007	+0.028	-0.028	-0.055	-20.5
5	+0.005	+0.006	-0.006	-0.061	-22.8
6	+0.018	+0.011	-0.011	-0.072	-26.8
7	+0.196	+0.107	-0.107	-0.179	-66.8
8	+0.16	+0.178	-0.178	-0.357	-133.2
9	-0.91	-0.38	+0.38	+0.023	+8.6
10	-0.233	-0.57	+0.57	+0.593	+221

Table 12. Calculation for normal stress σ_y across transverse section CG.

Station	σ_x fringes	p-q fringes	T_{xy} fringes	$\sqrt{(p-q)^2 - 4T_{xy}^2}$	σ_y fringes	σ_y p.s.i.
a	+0.994	3.36	0	-3.36	-2.37	-871
b	+0.99	3.4	0	-3.4	-2.41	-900
c	+0.98	3.5	0	-3.5	-2.52	-941
d	+0.85	3.7	0	-3.7	-2.85	-1065
e	+0.74	4.0	0	-4.0	-3.26	-1218
f	+0.674	4.5	0	-4.4	-3.82	-1425
g	+0.61	5.12	0	-5.12	-4.51	-1682
h	+0.593	6.18	-0.054	-6.18	-5.59	-2084

Table 13. Calculation for normal stress σ_y along horizontal section AC.

Station	σ_x fringes	p-q fringes	T_{xy} fringes	$\sqrt{(p-q)^2 - 4T_{xy}^2}$	σ_y fringes	σ_y p.s.i.
0	0	0.30	0	+0.30	+0.30	+112
1	-0.006	0.19	0	+0.19	+0.184	+ 69
2	-0.018	0.16	0	+0.16	+0.142	+ 53
3	-0.028	0.14	0	+0.14	+0.112	+ 42
4	-0.033	0.09	0	+0.09	+0.057	+ 21
5	-0.085	0.10	0	-0.10	-0.185	- 69
6	-0.071	0.5	0	-0.5	-0.571	-214
7	+0.114	1.1	0	-1.1	-0.986	-368
8	+0.454	2.0	0	-2.0	-1.546	-577
9	+0.834	2.85	0	-2.85	-2.016	-752
10	+0.994	3.3	0	-3.3	-2.306	-862

DISCUSSION

After the experimental work was done, it was interesting to compare the stress distribution along axis FC and CG (see Figs. 13 and 16) between the circular disk and the rectangular beam, because the isochromatic pattern of the circular disk under concentrated load is somewhat similar to that of the pinched rectangular beam.

The circular disk is sketched in Fig. 16, its diameter is equal to the depth of beam d .

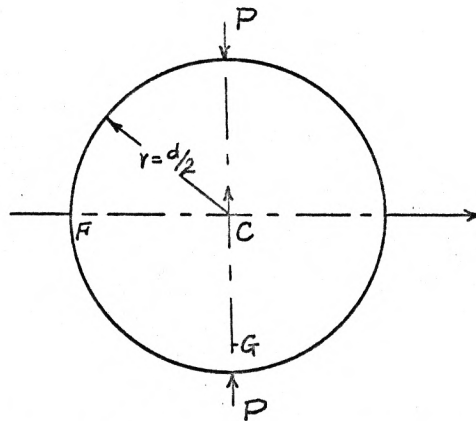


Fig. 16. Sketch showing circular disk under concentrated load P .

From the theoretical analysis of a circular disk under concentrated load, the rectangular stress components along the X axis are given as

$$\sigma_x = \frac{2p}{\pi t d} \left[\frac{d^2 - 4x^2}{d^2 + 4x^2} \right]^2$$

$$\sigma_y = - \frac{2p}{\pi t d} \left[\frac{4d^4}{(d^2 + 4x^2)^2} - 1 \right]$$

$$\tau_{xy} = 0$$

Along the Y axis

$$\sigma_x = \frac{2p}{\pi t d}$$

$$\sigma_y = - \frac{2p}{\pi t} \left[\frac{2}{d - 2y} + \frac{2}{d + 2y} - \frac{1}{d} \right]$$

$$\tau_{xy} = 0$$

where t is the thickness of circular disk, d diameter of disk and equal to 1.46 inch [2].

The values obtained from rectangular beam and circular disk are shown in Tables 14-17 and drawn on Figs. 17 and 18.

Table 14. Rectangular stress σ_x along line FC:

Station	5	6	7	8	9	10
psi						
Rectangular beam	-31.7	-26.5	42.5	169.0	312.0	370
Circular disk	0	73	156	240	306	331

Table 15. Rectangular stress σ_y along line FC:

Station	5	6	7	8	9	10
psi						
Rectangular beam	-69	-214	-368	-577	-752	-862
Circular disk	0	-151	-384	-653	-900	-993

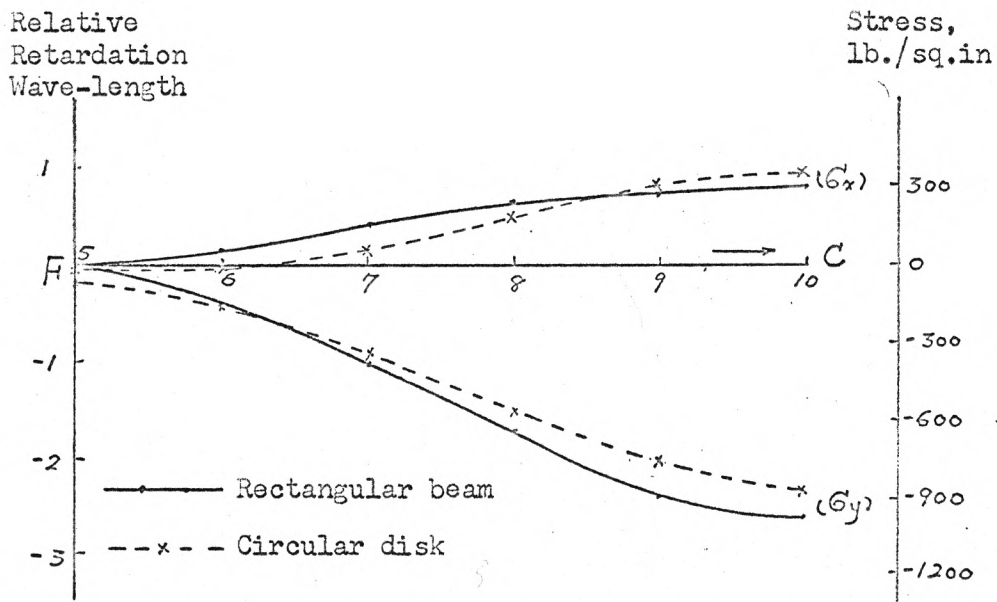


Fig. 17. Distribution of rectangular stress along FC.

Table 16. Rectangular stress σ_x along vertical line \overline{CG} .

Station	a	b	c	d	e	f	g	h
psi								
Rectangular beam	370.0	369	366	317	276	252	227.5	221
Circular disk	331	331	331	331	331	331	331	331

Table 17. Rectangular stress σ_y along vertical line \overline{CG} .

Station	a	b	c	d	e	f	g	h
psi								
Rectangular beam	-871	-900	-941	-1065	-1218	-1425	-1682	-2084
Circular disk	-993	-1008	-1048	-1124	-1250	-1425	-1740	-2265

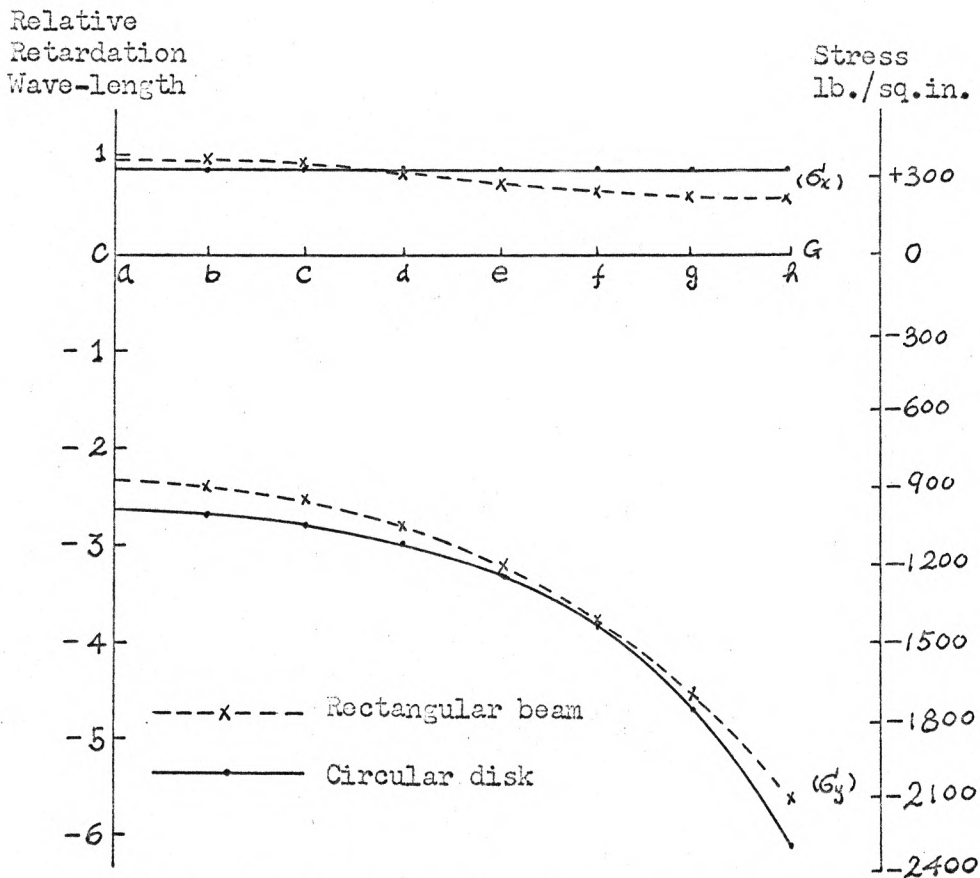


Fig. 18. Distribution of rectangular stress along CG.

CONCLUSION

There are several methods which can be used to evaluate the individual stresses according to the data obtained from application of the photoelastic technique. These include the relaxation method, shear difference method, the slope equilibrium method, etc. In this experiment, the shear difference method was employed to separate the stresses by using the data obtained from the isochromatic pattern and the isoclinic pattern.

It is known that to obtain an accurate isoclinic pattern is difficult, therefore, there are some possible errors in the numerical values after using the shear difference method. Along the curve MN of Fig. 11, which is a discrete set of isotropic points, all isoclinic lines from the middle part of the rectangular beam converge so, near this curve, there is a narrow range where the direction of principal stress changes abruptly and also, along this narrow range, the isoclinic lines are vague, therefore it is very hard to get accurate isoclinic lines near this region.

In order to get a good isoclinic pattern, care was taken to keep the applied load exactly on the symmetrical axis of the beam. It was also found necessary to vary the exposure time for different parts of the model if sharp isoclinic lines were to be obtained on all the photographs.

It would be interesting to compare the stress distribution for different kinds of rectangular beams which have different ratios of length to depth and applied loads of different width.

ACKNOWLEDGEMENTS

The writer wishes to express his thanks to Frank J. McCormick, Professor of Applied Mechanics, for his guidance and encouragement during the experimental work.

REFERENCES

1. Alexander, Nicholas, "Photoelasticity," Rhode Island State College Press, 1936.
2. Frocht, Max M. "Photoelasticity," Volume I and II, Wiley, New York, 1941 and 1948.
3. Heywood, R. E. "Designing by Photoelasticity," Chapman and Hall, London, 1949.
4. Jessup, H. T. and F. C. Harris. "Photoelasticity, Principles and Methods," Cleaver-Hume Press, London, 1949. (Also Dover reprint, 1960).
5. Lee, George Hamor, "An Introduction to Experimental Stress Analysis," Wiley, New York, 1962.

A PROBLEM IN PHOTOELASTICITY

by

TSU-JIUNN PENG

B. S., National Taiwan University, 1960

AN ABSTRACT OF A MASTER'S REPORT

submitted in partial fulfillment of the

requirements for the degree

MASTER OF SCIENCE

Department of Applied Mechanics

KANSAS STATE UNIVERSITY
Manhattan, Kansas

1964

The purpose of this experiment was to determine by photoelastic methods the principal stresses in a pinched rectangular beam along the vertical axis and the horizontal axis which are symmetrical lines of the beam. Photoelasticity is an optical phenomenon which is used as a method of experimental stress analysis.

The first step in this experiment was to select the material, make a rectangular beam and investigate the model under pinching loads through the polariscope. The next step was to separate the stress using the data obtained from the first step by means of the shear difference method. The results are discussed in the report by comparing the circular disk with the rectangular beam.

It was supposed that the stress distribution along the symmetrical axes of the rectangular beam were very close to that of the circular disk, but there is a small difference along the vertical axis. Whether it was induced by some numerical errors in the experimental data cannot be definitely stated without further investigation.